

A SEMI-EMPIRICAL TIGHT-BINDING THEORY OF THE ELECTRONIC STRUCTURE OF SEMICONDUCTORS†

P. VOGL

Institut für Theoretische Physik, Universität Graz, Graz, Austria

and

HAROLD P. HJALMARSON‡ and JOHN D. DOW

Department of Physics and Materials Research Laboratory, University of Illinois at Urbana-Champaign,
Urbana, IL 61801, U.S.A.

(Received 28 September 1981; accepted 19 November 1981)

Abstract—A nearest-neighbor semi-empirical tight-binding theory of energy bands in zincblende and diamond structure materials is developed and applied to the following sp^3 -bonded semiconductors: C, Si, Ge, Sn, SiC, GaP, GaAs, GaSb, InP, InAs, InSb, AlP, AlAs, AlSb, ZnSe, and ZnTe. For each of these materials the theory uses only thirteen parameters to reproduce the major features of conduction and valence bands. The matrix elements exhibit chemical trends: the differences in diagonal matrix elements are proportional to differences in free-atom orbital energies and the off-diagonal matrix elements obey the d^{-2} rule of Harrison *et al.* The lowest energy conduction bands are well described as a result of the introduction of an excited s state, s^* , on each atom. Examination of the chemical trends in this sp^3s^* model yields a crude but "universal" sp^3s^* model whose parameters do not depend explicitly on band gaps, but rather are functions of atomic energies and bond lengths alone. The "universal" model, although cruder than the sp^3s^* model for any single semiconductor, can be employed to study relationships between the band structures of different semiconductors; we use it to predict band edge discontinuities of heterojunctions.

1. INTRODUCTION

Now that semiconductors can be grown with varying composition a few atomic layers at a time [1], the number of conceivable new electronic devices and materials for improving the performance of existing devices will increase many-fold. This situation will put new demands on theorists to predict the properties of exotic semiconductors before the materials are even fabricated. This need to survey and simulate wide classes of semiconducting materials is not well met by most conventional theories, which concentrate on the accurate description of a few semiconductors. A notable exception, however, is the empirical Bond Orbital Model pioneered by Harrison [2, 3]; this model provides a simple nearest-neighbor tight-binding theory of valence bands and how they change as the chemistry of the semiconductor varies. With this model, one can estimate the nature of the filled, bonding valence bands of almost any semiconductor. However, a comparable model that also describes the empty anti-bonding conduction states is needed.

In this paper we present such a model. We maintain the spirit of Harrison's model of semiconductors by constructing a nearest-neighbor tight-binding theory which preserves and displays chemical trends, while successfully reproducing the unoccupied anti-bonding

lower conduction bands as well as the occupied bonding valence bands. In order to achieve these goals we have found, by trial and error, a chemically-correct tight-binding theory with a minimum number of parameters. We have replaced the actual semiconductor Hamiltonian with a pseudo-Hamiltonian [4] which (i) involves only a small number of localized pseudo-orbitals [5], (ii) has off-diagonal matrix elements that are significant only between states localized on adjacent sites, and (iii) has diagonal matrix elements that are determined by the free atom orbital energies of the semiconductor's chemical constituents and are only weakly influenced by the condensed-matter environment [6]. Such a replacement of the Hamiltonian was recently shown to produce an adequate pseudo-Hamiltonian [5, 6]. The resulting pseudo-orbital basis functions turn out to be atomic-like [6, 7]—although atomic orbitals themselves (as were used in early linear combination of atomic orbitals models) do not provide an adequate pseudo-Hamiltonian basis. The spirit of the pseudo-Hamiltonian replacement procedure is analogous to that of conventional empirical pseudopotential theory [8]: the matrix elements of the pseudo-Hamiltonian are adjusted to fit optical band gaps, thereby constraining the theory to produce a reasonable band structure.

Our model has all of the following properties: (i) the chemistry of sp^3 bonding is manifestly preserved; (ii) the diagonal matrix elements of the model are related to the atomic energies of the chemical constituents, permitting exploration of chemical trends, simple treatment of al-

†Please address reprint requests to Physics Department Reprint Secretary, Urbana.

‡Present address: Sandia National Laboratories, Division 5151, Albuquerque, NM 87185, U.S.A.

loys, and theories of semiconductors with defects; (iii) the off-diagonal matrix elements scale as the inverse square of the bond length (the d^{-2} scaling rule of the Bond Orbital Model [2,3]); (iv) the model employs a minimum number of parameters, only nearest-neighbor matrix elements; and (v) the theory successfully reproduces not only the valence bands but also the lowest conduction band, even in indirect gap semiconductors. Other empirical tight-binding theories lack one or more of these properties.

Theories with fewer than eight bands cannot describe the chemistry of localized states in covalently bonded semiconductors: the sp^3 bonding of zincblende and diamond structures demands a basis set of at least four orbitals for each of the two atoms in the unit cell, namely, one s and three p orbitals per atom. Tight binding theories with more than nearest-neighbor matrix elements have been discussed extensively in the classic paper of Slater and Koster [9]. For example, a zincblende structure with an sp^3 basis for each atom requires 9 and 23 independent parameters for first- and second-nearest-neighbor tight binding theories, respectively. In practice, attempts to determine extended-neighbor tight-binding parameters empirically are faced with so many adjustable parameters that least-squares fits [10] to pseudopotential bands are normally employed. The resulting parameters, although quite useful for a single semiconductor, cannot be confidently used to discuss different semiconductors, such as alloys, by interpolation, because the fitting procedure is insensitive to the chemistry and chemical trends in the band structure parameters. Moreover, the basic spirit of empirical tight-binding theory is to minimize the number of empirical parameters by restricting the number of non-zero matrix elements. Therefore, to preserve simplicity and to permit easy identification of chemical trends in the band structure, we limit our consideration to a nearest-neighbor tight-binding theory.

Attempts to fit the conduction bands of semiconductors with a nearest-neighbor sp^3 tight-binding model have generally failed; for example, Chadi *et al.* [11] showed that such a model cannot produce an indirect fundamental band gap in zincblende or diamond materials, and hence cannot adequately describe even the lowest conduction bands of such important semiconductors as Si, Ge, AlAs, or GaP. The nearest-neighbor sp^3 model fails to produce an indirect gap for Si because it omits essential physics: the excited atomic states, such as the s^* state of atomic Si, couple with the anti-bonding p -like conduction states of Si near the X and L points of the Brillouin zone, and press these states down in energy. The present theory overcomes this deficiency by including an excited s -state, s^* , on each atom, giving an sp^3s^* basis and a ten-band theory. The excited s^* state repels the lower, unoccupied energy levels of the neighboring atom, and, in particular, presses the indirect relative conduction band minima down in energy.

In an sp^3 -basis there are four diagonal matrix elements (s - and p -orbital energies for each atom) and five independent nearest neighbor transfer matrix elements ($V(s, s)$, $V(x, x)$, $V(x, y)$, $V(sa, pc)$, and $V(sc, pa)$).

These parameters all have physical significance; our procedure is to first determine them by fitting the pseudopotential bands [12], and then to augment the basis with the s^* state which, in this model, introduces a diagonal matrix element and off-diagonal matrix elements, only two of which we take to be non-zero: the couplings between s^* and p orbitals on adjacent sites. The reason for treating the s^* states *a posteriori* is that they are simply devices for producing accurate indirect band edges. The inclusion of some such excited states in any minimal basis set is physically important—although the precise physics of the actual excited states need not be faithfully and quantitatively reproduced. One would see this by executing a first-principles band calculation for a semiconductor: various excited states (including d states) must be introduced in order to obtain the correct band structure, because these excited states repel the energy levels below them, influencing the width of the conduction bands in particular. A central physical point of the present work is that any excited state that depresses the states below can be used to improve the sp^3 nearest-neighbor model conduction bands; therefore extensions of the model to distant-neighbor matrix elements (with the proliferation of adjustable matrix elements) can be avoided by introducing an s^* state.

In Section 2 we present the model Hamiltonian; the determination of its matrix elements is discussed in Section 3. The resulting matrix elements have scaling properties discussed in Section 4. Our results are summarized in Section 5. Appendix A contains the predicted band structures, and the remaining Appendices discuss details of the model.

2. MODEL HAMILTONIAN

We construct the zincblende-structure tight-binding Hamiltonian in a basis of quasi-atomic functions

$$|nb\mathbf{k}\rangle = N^{-1/2} \sum_{i,b} \exp(i\mathbf{k} \cdot \mathbf{R}_i + i\mathbf{k} \cdot \mathbf{v}_b) |nb\mathbf{R}_i\rangle. \quad (1)$$

The quantum numbers n run over the s , p_x , p_y , p_z , and s^* orbitals; the N wavevectors \mathbf{k} lie in the first Brillouin zone [13]; the site index b is either a (for anion) or c (for cation); the anion positions are \mathbf{R}_i ; and, in terms of the Kronecker δ , we have $\mathbf{v}_b = \delta_{b,c}(a/2)(1, 1, 1)$. The quasi-atomic functions are Löwdin orbitals: symmetrically orthogonalized atomic orbitals [14]. The Schrödinger equation for the Bloch functions $|k\lambda\rangle$ is

$$(H - \epsilon(k\lambda))|k\lambda\rangle = 0, \quad (2)$$

or, in this basis,

$$\sum_{m,b} \{ (nb\mathbf{k}|H|mb^*\mathbf{k}) - \epsilon(k\lambda)\delta_{n,m}\delta_{b,b^*} \} (mb^*\mathbf{k}|k\lambda\rangle = 0 \quad (3)$$

The solutions are

$$|k\lambda\rangle = \sum_{n,b} |nb\mathbf{k}\rangle (nb\mathbf{k}|k\lambda\rangle). \quad (4)$$

The band index λ has ten values. The Hamiltonian matrix in the $|nb\mathbf{k}\rangle$ basis is:

Table (A)

	$ sa\rangle$	$ sc\rangle$	$ p_xa\rangle$	$ p_ya\rangle$	$ p_xa\rangle$	$ p_ya\rangle$	$ p_xc\rangle$	$ p_yc\rangle$	$ p_xc\rangle$	$ p_yc\rangle$	$ s^*a\rangle$	$ s^*c\rangle$
$ sa\rangle$	$E(s,a)$	$V(s,s)g_0$	0	0	0	0	$V(sa,pc)g_1$	$V(sa,pc)g_2$	$V(sa,pc)g_3$	0	0	0
$ sc\rangle$	$V(s,s)g_0^*$	$E(s,c)$	$-V(pa,sc)g_1^*$	$-V(pa,sc)g_2^*$	$-V(pa,sc)g_3^*$	0	0	0	0	0	0	0
$ p_xa\rangle$	0	$-V(pa,sc)g_1$	$E(p,a)$	0	0	$V(x,x)g_0$	$V(x,y)g_3$	$V(x,y)g_2$	$V(x,y)g_1$	0	0	$-V(pa,s^*c)g_1$
$ p_ya\rangle$	0	$-V(pa,sc)g_2$	0	$E(p,a)$	0	$V(x,y)g_3$	$V(x,x)g_0$	$V(x,y)g_2$	$V(x,y)g_1$	0	0	$-V(pa,s^*c)g_2$
$ p_xc\rangle$	0	$-V(pa,sc)g_3$	0	0	$E(p,a)$	$V(x,y)g_2$	$V(x,x)g_1$	$V(x,y)g_0$	0	0	0	$-V(pa,s^*c)g_3$
$ p_xc\rangle$	$V(sa,pc)g_1^*$	0	$V(x,x)g_0^*$	$V(x,y)g_3^*$	$V(x,y)g_2^*$	$E(p,c)$	0	0	0	0	$V(s^*a,pc)g_1^*$	0
$ p_yc\rangle$	$V(sa,pc)g_2^*$	0	$V(x,y)g_3^*$	$V(x,x)g_0^*$	$V(x,y)g_1^*$	0	0	$E(p,c)$	0	0	$V(s^*a,pc)g_2^*$	0
$ p_zc\rangle$	$V(sa,pc)g_3^*$	0	$V(x,y)g_2^*$	$V(x,y)g_1^*$	$V(x,x)g_0^*$	0	0	0	$E(p,c)$	0	$V(s^*a,pc)g_3^*$	0
$ s^*a\rangle$	0	0	0	0	0	$V(s^*a,pc)g_1$	$V(s^*a,pc)g_2$	$V(s^*a,pc)g_3$	0	0	$E(s^*,a)$	$V(s^*,s^*)g_0$
$ s^*c\rangle$	0	0	$-V(pa,s^*c)g_1^*$	$-V(pa,s^*c)g_2^*$	$-V(pa,s^*c)g_3^*$	0	0	0	0	0	$V(s^*,s^*)g_0^*$	$E(s^*,c)$

where we have

$$g_0(\mathbf{k}) = \cos(k_1 a_L/4) \cos(k_2 a_L/4) \cos(k_3 a_L/4) - i \sin(k_1 a_L/4) \times \sin(k_2 a_L/4) \sin(k_3 a_L/4),$$

$$g_1(\mathbf{k}) = -\cos(k_1 a_L/4) \sin(k_2 a_L/4) \sin(k_3 a_L/4) + i \sin(k_1 a_L/4) \times \cos(k_2 a_L/4) \cos(k_3 a_L/4),$$

$$g_2(\mathbf{k}) = -\sin(k_1 a_L/4) \cos(k_2 a_L/4) \sin(k_3 a_L/4) + i \cos(k_1 a_L/4) \times \sin(k_2 a_L/4) \cos(k_3 a_L/4),$$

and

$$g_3(\mathbf{k}) = -\sin(k_1 a_L/4) \sin(k_2 a_L/4) \cos(k_3 a_L/4) + i \cos(k_1 a_L/4) \times \cos(k_2 a_L/4) \sin(k_3 a_L/4). \tag{6}$$

The independent tight-binding matrix elements, to be determined by fitting band structure data, are expressed in the localized Lowdin basis of symmetrically orthogonalized atomic orbitals $|nbR\rangle$:

$$E(s, b) = (sbR|H|sbR),$$

$$E(p, b) = (p_x bR|H|p_x bR),$$

$$V(s, s) = 4(saR|H|scR),$$

$$V(x, x) = 4(p_x aR|H|p_x cR),$$

$$V(x, y) = 4(p_x aR|H|p_y cR),$$

$$V(sa, pc) = 4(saR|H|p_x cR),$$

and

$$V(pa, sc) = 4(p_x aR|H|scR). \tag{7}$$

Here we have $b = a$ (anion) or $b = c$ (cation). The above nine parameters, four diagonal energies and five transfer matrix elements V , determine the band structure in a nearest-neighbor, sp^3 , eight-band model. We include an excited s state, s^* , in our ten-band $sp^3 s^*$ model, and permit only coupling to p -states on adjacent sites, omitting, for simplicity, the coupling to s -states on different sites [15]. Thus we have four additional matrix elements, two diagonal energies and two transfer matrix elements

$$E(s^*, b) = (s^* bR|H|s^* bR),$$

$$V(s^* a, pc) = 4(s^* aR|H|p_x cR),$$

and

$$V(pa, s^* c) = 4(p_x aR|H|s^* cR). \tag{8}$$

The empirical matrix elements are given in Table 1, and the band structure data used in determining them are given in Table 2.

Table 1. Empirical matrix elements of the $sp^3 s^*$ Hamiltonian in eV. Although only three digits are significant, we reproduce the actual numbers used to generate the figures in order to eliminate any problem with round-off errors

Compound	$E(s, a)$	$E(p, a)$	$E(s, c)$	$E(p, c)$	$E(s^*, a)$	$E(s^*, c)$
C	-4.5450	3.8400	-4.5450	3.8400	11.3700	11.3700
Si	-4.2000	1.7150	-4.2000	1.7150	6.6850	6.6850
Ge	-5.8800	1.6100	-5.8800	1.6100	6.3900	6.3900
Sn	-5.6700	1.3300	-5.6700	1.3300	5.9000	5.9000
SiC	-8.4537	2.1234	-4.8463	4.3466	9.6534	9.3166
AlP	-7.8466	1.3169	-1.2534	4.2831	8.7069	7.4231
AlAs	-7.5273	0.9833	-1.1627	3.5867	7.4833	6.7267
AlSb	-6.1714	0.9807	-2.0716	3.0163	6.7607	6.1543
GaP	-8.1124	1.1250	-2.1976	4.1150	8.5150	7.1850
GaAs	-8.3431	1.0414	-2.6569	3.6686	8.5614	6.7569
GaSb	-7.9207	0.8554	-3.8993	2.9146	6.6354	5.9846
InP	-8.5274	0.8735	-1.4826	4.0465	8.2635	7.0665
InAs	-9.5381	0.9099	-2.7219	3.7201	7.4099	6.7401
InSb	-8.0157	0.6738	-3.4643	2.9162	6.4530	5.9362
ZnSe	-11.8383	1.5072	0.0183	5.9928	7.5872	8.9928
ZnTe	-9.8150	1.4834	0.9350	5.2666	7.0834	8.2666
GaSb	-7.1256	0.6718	-3.3042	2.7312	6.6354	5.4846

Compound	$V(s, s)$	$V(x, x)$	$V(x, y)$	$V(sa, pc)$	$V(sc, pa)$	$V(s^* a, pc)$	$V(pa, s^* c)$	$V(sa, pc)$	$V(sc, pa)$	$V(s^* a, pc)$	$V(pa, s^* c)$
C	-22.7250	3.8400	11.6700	15.2206	15.2206	8.2109	8.2109				
Si	-8.3000	1.7150	4.5750	5.7292	5.7292	5.3749	5.3749				
Ge	-6.7800	1.6100	4.9000	5.4649	5.4649	5.2191	5.2191	4.9617	4.9617	4.5434	4.5434
Sn	-5.6700	1.3300	4.0800	4.3286	4.3286	3.9665	3.9665	4.2288	4.2288	3.9665	3.9665
SiC	-12.4197	3.0380	5.9216	9.4900	9.2007	8.7138	4.4051				
AlP	-7.4535	2.3749	4.8378	5.2451	5.2775	5.2508	4.6388				
AlAs	-6.6642	1.8780	4.2919	5.1106	5.4965	4.5216	4.9950				
AlSb	-5.6448	1.7199	3.6648	4.9121	4.2137	4.3662	3.0739				
GaP	-7.4709	2.1516	5.1369	4.2771	6.3190	4.6541	5.0950				
GaAs	-6.4513	1.9546	5.0779	4.4000	5.7099	4.8422	4.8072	4.2485	5.2671	4.7515	4.2547
GaSb	-6.1567	1.5789	4.1285	4.9601	4.6675	4.9895	4.2180				
InP	-5.3614	1.8801	4.2324	2.2265	5.5825	3.4623	4.4814				
InAs	-5.6052	1.8398	4.4693	3.0354	5.4389	3.3744	3.9097				
InSb	-5.5193	1.4018	3.8761	3.7880	4.5900	3.5666	3.4048				
ZnSe	-6.2163	3.0054	5.9942	3.4980	6.3191	2.5891	3.9533				
ZnTe	-6.5765	2.7951	5.4670	5.9827	5.8199	1.3196	0.0000				
GaSb	-5.9854	1.3546	4.4438	6.1643	4.4708	5.1604	4.1144				

Table 2. Bond lengths d (in Angstroms) and band structure energies at symmetry points (zincblende notation) in eV

Compound	d	eV								Reference
		Γ_1^v	Γ_1^c	Γ_{15}^c	X_1^v	X_3^v	X_5^v	X_1^c	X_3^c	
C	1.54	-27.27	18.18	7.68	-16.14	-16.14	-7.83	5.48	5.48	{a} {b}
Si	2.35	-12.50	4.10	3.43	-7.69	-7.69	-2.86	1.13	1.13	{b} {c}
Ge	2.45	-12.66	0.90	3.22	-8.66	-8.66	-3.29	1.46	1.46	{b} {c}
Sn	2.81	-11.34	0.00	2.66	-7.88	-7.88	-2.75	0.90	0.90	{c}
SiC	1.88	-19.20	5.90	6.47	-13.50	-11.20	-2.79	2.33	5.41	{d}
AlP	2.36	-12.70	3.60	5.60	-9.80	-5.40	-2.26	2.50	3.00	{e} {f}
AlAs	2.45	-11.73	3.04	4.57	-9.52	-5.69	-2.20	2.30	2.68	{g} {h}
AlSb	2.66	-10.13	1.88	4.00	-8.30	-5.03	-1.80	1.98	2.41	{i} {j}
GaP	2.36	-13.19	2.88	5.24	-9.46	-7.07	-2.73	2.35	2.90	{c} {k}
GaAs	2.45	-12.55	1.55	4.71	-9.83	-6.88	-2.89	1.95	2.38	{b} {c}
GaSb	2.64	-11.64	0.84	3.70	-9.62	-6.90	-2.95	1.43	1.20	{l} {m}
InP	2.54	-11.42	1.41	4.92	-8.91	-6.01	-2.06	2.44	2.97	{c} {g}
InAs	2.62	-12.69	0.43	4.63	-10.20	-6.64	-2.37	2.28	2.66	{c} {g}
InSb	2.81	-11.71	0.23	3.59	-9.20	-6.43	-2.24	1.71	1.83	{c} {g}
ZnSe	2.45	-14.50	2.68	7.50	-12.50	-5.60	-2.65	4.54	5.17	{b} {l}
ZnTe	2.64	-13.31	2.56	6.75	-11.90	-5.67	-2.41	5.97	6.24	{b} {l}

- {a} N. E. Brenev, Phys. Rev. B 11, 919 (1975).
- {b} J. C. Phillips, Bonds and Bands in Semiconductors (Academic Press, New York, (1973)).
- {c} J. R. Chelikowsky and M. L. Cohen, Phys. Rev. B 14, 556 (1976).
- {d} L. A. Hemstreet, Jr. and C. Y. Fong, Solid State Commun. 9, 643 (1971).
- {e} P. Vogl, unpublished.
- {f} J. I. Pankove, Optical Processes in Semiconductors, (Prentice-Hall, Englewood Cliffs, New Jersey, 1971).
- {g} R. C. Weast and M. J. Astle, Eds., CRC Handbook of Chemistry and Physics, 59th Edition, (CRC Press, Inc., Palm Beach, Florida, 1978).
- {h} A. Baldereschi, E. Hess, K. Maschke, H. Neumann, K. R. Schulze, and K. Unger, J. Phys. C 10, 4709 (1977).
- {i} M. L. Cohen and T. K. Bergstresser, Phys. Rev. 141, 789 (1966).
- {j} M. Cardona, J. Appl. Phys. Suppl. 32, 2151 (1961); T. E. Fischer, Phys. Rev. 139, A1228 (1965); and M. Cardona, F. H. Pollak, and K. L. Shaklee, Phys. Rev. Letters, 16, 644 (1975).
- {k} M. B. Sturge, R. T. Vink, F. P. J. Kuijpers, Appl. Phys. Letters 32, 49 (1978).
- {l} D. J. Chadi, unpublished.
- {m} T. C. Chiang, D. E. Eastman, Phys. Rev. B 22, 2940 (1980)

3. DETERMINATION OF THE MATRIX ELEMENTS OF H

(a) The sp^3 model

In selecting a scheme for determining the matrix elements, we concentrate on producing energy bands which mimic the nonlocal pseudopotential bands [12], and, in particular, reproduce the spectral densities of states. The reason for paying close attention to the densities of states is our desire to employ the empirical Hamiltonian for localized defect calculations; such computations are extremely sensitive to minor redistributions of state density [16-18].

For clarity of presentation, we discuss only GaP in the main text, leaving the discussion of other semiconductors to Appendix A. We eschew least-squares methods [10] of fitting the bands in favor of careful treatment of the $\mathbf{k} = 0$ Γ -point and the $\mathbf{k} = (2\pi/a_1)(1, 0, 0)$ X -point of the Brillouin zone. (The highest valence band maximum of GaP is at Γ and the lowest conduction minima are at X .) In terms of the band energies at X and Γ (see Fig. 1), we have expressions for the tight-binding matrix elements as functions of the diagonal energies $E(1, c)$ and $E(1, a)$:

$$V(s, s) = (1/2) \{ [E(\Gamma_1^c) - E(\Gamma_1^v)]^2 - [E(s, c) - E(s, a)]^2 \}^{1/2}$$

$$V(x, x) = (1/2) \{ [E(\Gamma_{15}^c) - E(\Gamma_{15}^v)]^2 - [E(p, c) - E(p, a)]^2 \}^{1/2}$$

$$V(x, y) = (1/2) \{ [E(\Gamma_1^c) - 2E(X_5^v)]^2 - [E(p, c) - E(p, a)]^2 \}^{1/2}$$

$$V(sa, pc) = (1/2) \{ [E(s, a) + E(p, c) - \sqrt{2}E(X_1^v)]^2 - [E(s, a) - E(p, c)]^2 \}^{1/2}$$

and

$$V(pa, sc) = (1/2) \{ [E(s, c) + E(p, a) - \sqrt{2}E(X_3^v)]^2 - [E(s, c) - E(p, a)]^2 \}^{1/2} \tag{9}$$

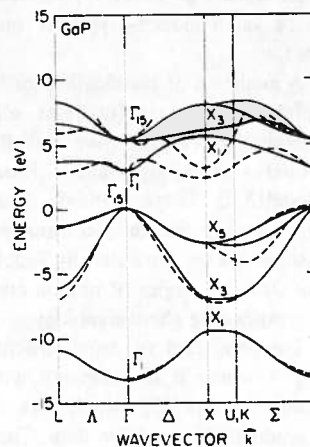


Fig. 1. The sp^3 (solid) and pseudopotential (dashed; Ref. [12]) band structures of GaP.

The sums of diagonal energies are related to the energies at Γ :

$$E(s, c) + E(s, a) = E(\Gamma_1^v) + E(\Gamma_1^c),$$

and

$$E(p, c) + E(p, a) = E(\Gamma_{15}^v) + E(\Gamma_{15}^c). \quad (10)$$

Seven of these nine energies are fixed by the band structure at seven points: Γ_1 , Γ_{15} , X_1 , X_3 , and X_5 in the valence band, and Γ_1 and Γ_{15} in the conduction band. (Note that the pseudopotential band structure is normally fit to reflectivity and photoemission data. Thus, by adjusting our tight-binding model to fit that band structure, we are, in reality, fitting the primary data.)

The remaining two energies are determined by fixing the differences in diagonal matrix elements:

$$D_1 = E(1, c) - E(1, a). \quad (11)$$

These are assumed to be functions of the atomic orbital energies $w(1, b)$ of Table 3. Expanding D_1 to lowest order in the neutral atom energies and recognizing that $D_1 = 0$ for homonuclear semiconductors, we find

$$D_1 = E(1, c) - E(1, a) = \beta_1(w(1, c) - w(1, a)). \quad (12)$$

The constants β_1 should be nearly equal for a variety of zincblende hosts, because the elements forming the zincblende compounds are all chemically similar (especially the III-V's). Indeed, we find $\beta_s = 0.8$ and $\beta_p = 0.6$ using the procedures of Appendix B. These last two constraints serve to completely determine the parameters of the sp^3 band structure.

A crucial test for the internal consistency of the model is provided by the amount of charge transferred from the cation to the anion. The same diagonal matrix elements can be used for an atom in different chemical environments only if the pseudoatoms are nearly neutral entities. Once we have fixed the Hamiltonian parameters, we calculate the net charge per anion or cation by performing an energy integral over valence band states of the local density of states [19] per atom. We find this charge to be small indeed—typically one-tenth of an electron charge.

A modicum of justification for the assumption that the differences D_1 are functions solely of atomic orbital energies is available from Bullett's chemical pseudopotential theory [6] and Harrison's Bond-Orbital Model [2, 3]. These methods of atomic and solid-state physics show that the electronic properties of an atom in a solid can be simulated by functions which depend on the atomic energies of neutral atoms; we are adopting a corresponding phenomenology.

The computed sp^3 band structure for GaP is given in Fig. 1 where it is compared with the pseudopotential band structure [12], which was empirically adjusted to reproduce the available data. The valence bands of the sp^3 model are good but the lowest conduction band, which has too much dispersion, does not have minima near the X points of the Brillouin zone.

(b) The sp^3s^* model

To remedy this deficiency of the sp^3 model, we add an excited s state to the basis, and couple it to the p states in such a way that it can reduce the dispersion in the conduction band and drive the relative minima at X to lower energy (Fig. 2). This s^* state is actually an *ad hoc* device that permits adjustment of the lowest conduction band near X (and also near L). Addition of s^* is simpler than augmenting the basis with d orbitals, which would necessitate treatment of higher angular momentum states and the development of unique empirical prescriptions for d matrix elements. The addition of an excited state to the basis set is to be preferred over extension of the model to second and more distant neighbors because the repulsion of the conduction band by the excited state plays a central role in fixing the indirect gaps. Economy of parameters also argues against the proliferation of comparably sized matrix elements associated with allowance for second-nearest-neighbor interactions.

The expected s^* states are allowed to interact only with the p states on the nearest neighbor atom. The s^* states, being at higher energy, repel the p -like conduction band levels near X and L downward in energy, producing the desired indirect band structure.

The excited s^* state energies $E(s^*)$ listed in Table 3 were derived from spectroscopic energy levels by averaging over multiplets of angular momentum, as described in Appendix C.

The coupling of the s^* states to the p -state is chosen to reproduce the X -point energy of each of the two lowest conduction bands. For the zincblende lattice, $V(s^*a, pc)$ is adjusted to fit the X_1^c energy and

Table 3. Atomic orbital energies in eV for atoms from Columns II-VI of the periodic table, taken from Refs. [32, 33]

Element	$-w(s)$	$-w(p)$	$-w(s^*)$
Be	8.4121	5.0500	
B	13.4560	8.4281	
C	19.1932	11.7868	4.26
N	25.7130	15.4388	4.99
O	33.8454	17.1877	7.94
F	42.7729	19.8564	
Mg	6.8831	3.7600	
Al	10.7011	5.7106	2.57
Si	14.6840	8.0814	3.11
P	18.9425	10.6544	3.27
S	23.9232	11.8963	5.27
Cl	29.1832	13.7740	
Zn	7.9563	3.4816	
Ga	11.5490	5.6712	2.60
Ge	15.0520	7.8156	3.04
As	18.6568	10.0497	3.55
Se	22.5771	10.9575	4.89
Br	27.0011	12.4327	
Cd	7.2043	2.9920	
In	10.1366	5.3661	2.34
Sn	12.9598	7.2089	2.64
Sb	15.8258	9.1033	3.33
Te	19.0563	9.7870	4.19
I	22.3347	10.9665	
Hg	7.1008	1.4960	
Tl	9.8226	5.2332	
Pb	12.4107	6.9520	
Bi	15.0051	8.7039	3.50
Po	17.9022	9.2847	
At	20.8189	10.3324	

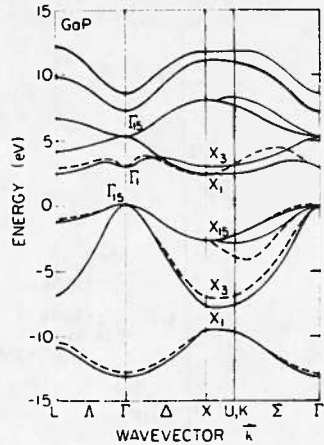


Fig. 2. The sp^3s^* model band structure (solid) compared with the pseudopotential (dashed: Ref. [12]) band structure of GaP.

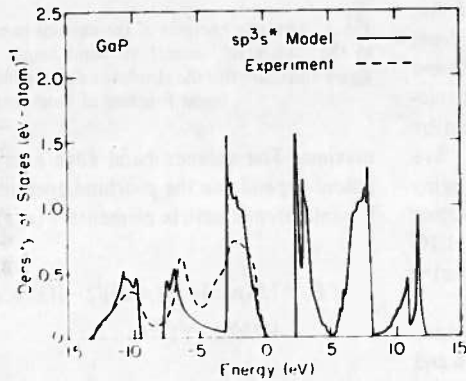


Fig. 3. Comparison of the sp^3s^* model density of states with the photoemission data of Ref. [23].

$V(pa, s^*c)$ is fixed to fit the X_3^c energy. The parameters of the sp^3 model are retained without alteration; the two parameters listed above would be zero in the sp^3 model [22].

The resulting sp^3s^* band structure is in good agreement with the pseudopotential band structure (Fig. 2) and the density of states agrees with the photoemission data [23] (Fig. 3).

4. SCALING PROPERTIES OF THE MATRIX ELEMENTS AND THE UNIVERSAL MODEL

(a) Scaling properties of matrix elements

To a good approximation, the off-diagonal matrix elements determined in the sp^3 model have the d^{-2} scaling law of the Bond Orbital Model (see Fig. 4), where d is the bond length ($d = \sqrt{3}a_c/4$). This property is extremely useful for treating lattice relaxation around defects or at surfaces, because it gives prescriptions for the matrix elements in the relaxed material in terms of the perfect crystal matrix elements.

The differences in diagonal matrix elements $E(1, c) - E(1, a)$, by construction, are proportional to the differences in atomic energies $w(1, c) - w(1, a)$.

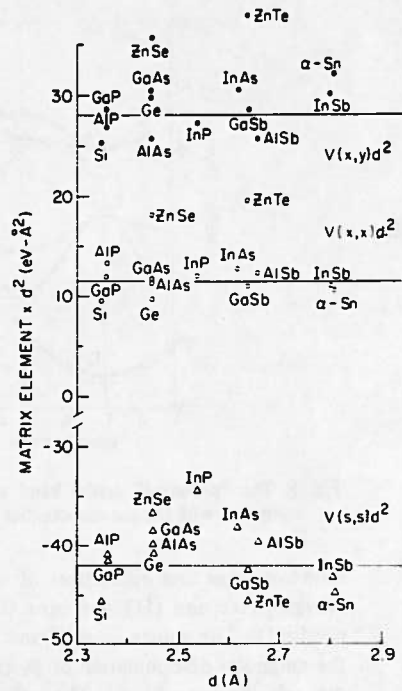


Fig. 4. Interatomic matrix elements $V(s, s)$, $V(x, x)$ and $V(x, y)$ multiplied by the square of the bond length vs the bond length d . This illustrates the d^{-2} scaling law. Semiconductors with small bond lengths, C and SiC, are off the scale of this figure.

Moreover, the excited s^* state matrix elements exhibit little variation from one semiconductor to another. (See Table 3).

(b) The "universal" model

Except for the sums of diagonal matrix elements, $E(1, c) + E(1, a)$, which have not yet been related to atomic energies or bond lengths, the sp^3s^* model has all of its matrix elements approximately fixed by the atomic energies of the constituents and a set of "universal" constants. In other words, this work suggests that all zincblende and diamond semiconductors have electronic structures that can be predicted crudely from a simple "universal" model of the energy bands, which involves only atomic energies and a set of universal off-diagonal matrix elements.

To formulate a "universal" model, we attempt to directly relate the sums $E(1, c) + E(1, a)$ to atomic energies. We find, in analogy with eqn (11), that, to a satisfactory approximation:

$$E(1, c) + E(1, a) = \{1 + \alpha_1\} \{w(1, c) + w(1, a)\}.$$

A modicum of justification for this form of a relationship between the energies in the solid and in the atom is given in Appendix D.

Thus we have the following "universal" model of semiconductor electronic structure whose matrix elements for each semiconductor depend solely on the neutral-atom orbital energies of its constituents and its lattice constant. The diagonal matrix elements, which represent orbital energies within the solid, are defined in

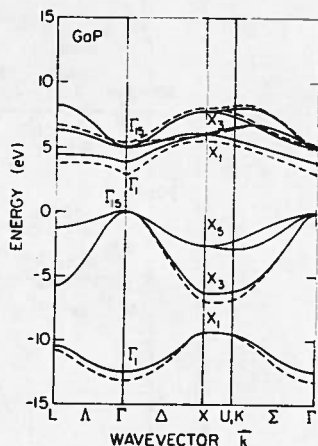


Fig. 5. The "universal" model band structure of GaP (solid) compared with the pseudopotential results of Ref. [12].

terms of sums and differences of neutral atomic orbital energies (see eqn (11) and eqns (D3) and (D4) of Appendix D). The values $\alpha_s = 0.2$ and $\alpha_p = 0.4$ follow from the empirical determination of β_1 (see Appendix B) and the relation $\alpha_1 = 1 - \beta_1$. The off-diagonal matrix elements, also known as transfer energies, are obtained by the d^{-2} scaling rule: $V(i) = V^0(i)d^{-2}$. The five coefficients $V^0(i)$ (see Fig. 4) were obtained by averaging over the semiconductors listed in Table 1. The resulting coefficients in eV, are $V^0(s, s) = -42.15$, $V^0(x, x) = 11.19$, $V^0(x, y) = 27.88$, $V^0(sa, pc) = 29.61$, and $V^0(sc, pa) = 33.76$.

The universal model accurately simulates the valence band energies and spectral densities of states (Figs. 6 and 7). The center of the conduction bands and their general features (lowest-energy moments) are also reproduced. However, the detailed features of the band structure, such as the optical bandgap, are not very accurately predicted. In addition to the broad features of the valence bands, the absolute energy placements, with respect to the vacuum reference, of the valence and conduction band edges are predicted.

Predictions of the discontinuities of the valence band edges are directly made with the universal model, which estimates the absolute energies of the valence band

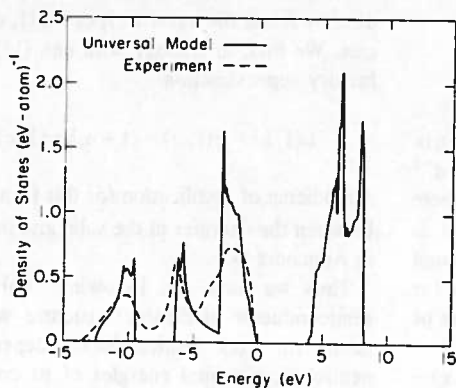


Fig. 6. The density of states of the "universal" model of GaP (solid) compared with the data of Ref. [23].

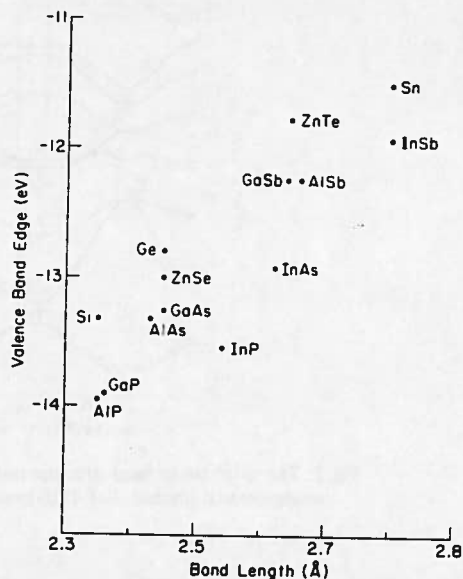


Fig. 7. Absolute energies of the valence band maxima calculated in the "universal" model vs bond length in Angstroms. This figure illustrates that the absolute valence band maxima are nearly a linear function of bond length.

maxima. The valence band edge energy for each compound depends on the p -orbital energies of its atoms and the interatomic matrix elements $V(x, x) = V^0(x, x)d^{-2}$:

$$E_v = [E(p, c) + E(p, a)]/2 - [(E(p, c) - E(p, a))^2 + 4V(x, x)^2]^{1/2}/2.$$

Using the equilibrium bond length d for each compound, we predict E_v and find that it is nearly a linear function of the bond length (Fig. 7). Such a linear trend with bond length suggests that experimenters' efforts to match lattice constants of the alloys used in heterojunctions may also serve to nearly match valence band edges as well. That remains a useful strategy even though the band discontinuity of any specific lattice-matched heterostructure does not become exactly zero either in our theory or in the data. One should focus on the general trend displayed in Fig. 7, which clearly demonstrates that lattice-matched heterojunctions tend to have small valence band discontinuities.

The predictions of band-discontinuities at hetero-junction interfaces can be made directly from Fig. 7. The bandstructure discontinuity of the valence band, $\delta E(A, B) = E(\Gamma_{15}^v; A) - E(\Gamma_{15}^v; B)$, is obtained from the maximum valence band energies, $E(\Gamma_{15}^v; A)$ and $E(\Gamma_{15}^v; B)$, of the two interfaced semiconductors. The conduction band discontinuity $\delta E(A, B)_c$ follows from the known bandgaps of these two semiconductors. Our values for the Ge/Si and the Ge/GaAs interfaces, two of the few that have been measured and published, are within 0.5 eV agreement of the published data and other theoretical estimates (see Table 5). Predictions for other interfaces can be made by examining Fig. 7. For instance, AlAs and GaAs have very similar lattice constants, and thus their valence band discontinuity is small:

Table 4. Spin-orbit parameters in eV (a)

Compound	Δ_0	Δ_a	Δ_c
AlAs	0.28	0.421	0.024
AlP	0.10	0.067	0.024
GaAs	0.34	0.421	0.174
GaP	0.10	0.067	0.174
GaSb	0.80	0.973	0.179
InAs	0.41	0.421	0.392
InP	0.14	0.067	0.392
InSb	0.28	0.973	0.392
ZnSe	0.45	0.48	0.074

(a) D. J. Chadi, Phys. Rev. B16, 790 (1977), and references therein. The values of Δ_0 in this reference are similar to more recently determined values of K. C. Rustagi, P. Merle, D. Auvergne, and H. Mathieu, Solid State Commun. 13, 1201 (1976).

Table 5. Band edge discontinuities in eV

Ge/Si	
Bond orbital model	0.38 (a)
Universal model	0.45
Experiment	0.24 to 0.17 (b)
Ge/GaAs	
Bond orbital model	0.41 (a)
Pseudopotential theory	0.35 (c)
Universal model	0.50
Experiment	0.36 to 0.76 (d)

(a) Ref. [2][3]
 (b) A. G. Milnes and D. L. Feucht, Heterojunctions and Metal-Semiconductor Junctions, (Academic Press, New York, 1972).
 (c) W. E. Pickett, S. G. Louie, and M. L. Cohen, Phys. Rev. B17, 815 (1978).
 (d) R. Dingle, W. Wiegmann, and C. H. Henry, Phys. Rev. Letters 33, 827 (1974).

$\delta E(\text{AlAs, GaAs}) \approx -0.1 \text{ eV}$. Similarly, $\delta E(\text{Ge, ZnSe}) \approx 0.2$ and $\delta E(\text{GaAs, ZnSe}) \approx -0.25$ because Ge, GaAs and ZnSe have similar lattice constants [24]. Such agreement, which is quite good on the $\sim 20 \text{ eV}$ scale of the physics determining δE [18] provokes us to investigate other

possible interfaces to determine those which will provide an interface with matched valence bands and lattice constants.

We hope that this will stimulate experimenters to establish the connections among lattice mismatch, atomic energies, and band edge discontinuities at heterojunctions.

SUMMARY

In summary, we have developed an sp^3s^* empirical nearest-neighbor tight-binding model that reproduces the valence and conduction band structures of major semiconductors.

In separate work we have successfully applied this model to several problems. These include the following: the theory of deep impurity levels in homopolar and heteropolar semiconductors and semiconductor alloys [17]; the theory of core excitons in the bulk [25], at interfaces [26], and at surfaces [27]; surface state theory [28]; models of deep traps at interfaces [29] and lattice-relaxed surfaces [30]; and a theory of extended, paired substitutional defects [31].

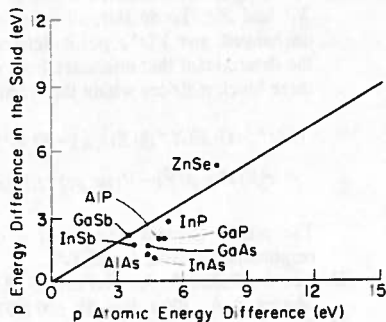


Fig. 8. The p -orbital energy differences, obtained from eqn (B1) vs the p -orbital energy differences for neutral atoms. The slope of the dashed line is $\beta_p = 0.6$.

The "universal" model extracted as an approximation to the sp^3s^* model promises to be a useful model for global theoretical studies of chemical trends in semiconductors; for example, estimates of the band discontinuities as a function of lattice mismatch for heterojunctions.

Acknowledgements—We gratefully acknowledge stimulating conversations with J. D. Joannopoulos, D. J. Chadi, W. A. Harrison, D. J. Wolford, and W. Y. Hsu and the support of the Department of Energy through the Illinois Materials Research Laboratory (DE-AC02-76ER01198), the Office of Naval Research (ONR-N-00014-77-C-0537), and the Fonds zur Förderung der wissenschaftlichen Forschung in Österreich (Projekt Nr. 4236).

REFERENCES

- Arthur J. R., *J. Appl. Phys.* **39**, 4032 (1968); Cho A. Y., *J. Vac. Sci. Technol.* **8**, 531 (1971); Matthews J. W. and Blakeslee A. E., *J. Crystal Growth* **27**, 118 (1974); **29**, 273 (1975); **32**, 265 (1976); Esaki L. and Chang L. L., *Crit. Rev. Solid State Sci.* **6**, 195 (1976).
- Harrison W. A., *Phys. Rev.* **B8**, 4487 (1973); Harrison W. A. and Ciraci S., *Phys. Rev.* **B10**, 1516 (1974); Pantelides S. T. and Harrison W. A., *Phys. Rev.* **B11**, 3006 (1975).
- Harrison W. A., *Electronic Structure and the Properties of Solids*. Freeman, San Francisco (1980).
- The basic philosophy of this pseudo-Hamiltonian approach in a tight-binding basis is borrowed from the early k -space pseudopotential studies designed to produce the "smoothest" and most plane-wave-like pseudowavefunction. See, for example, Austin B. J., Heine V. and Sham L. J., *Phys. Rev.* **127**, 276 (1962).
- Louie S. G., *Phys. Rev.* **B22**, 1933 (1980).
- Bullett D. W., *J. Phys.* **C8**, 2695, 2707 (1975); *Solid State Physics* (Edited by H. Ehrenreich, F. Seitz, and D. Turnbull), Vol. 35, p. 129. Academic Press, New York (1980); V. Heine, *Ibid.* p. 1.
- Kane E. O. and Kane A. B., *Phys. Rev.* **B17**, 2691 (1978); Tejedor C. and Verges J. A., *Phys. Rev.* **B19**, 2283 (1979).
- Cohen M. L. and Heine V., *Solid State Physics* (Edited by H. Ehrenreich, F. Seitz and D. Turnbull), Vol. 24, pp. 38–248. Academic Press, New York (1970).
- Slater J. C. and Koster G. F., *Phys. Rev.* **94**, 1498 (1954).
- Dresselhaus G. and Dresselhaus M. S., *Phys. Rev.* **160**, 6491 (1967); Pandey K. C. and Phillips J. C., *Phys. Rev.* **B13**, 750 (1976); Schulman J. N. and McGill T. C., *Phys. Rev.* **B19**, 6341 (1979); Daw M. S. and Smith D. L., *J. Vac. Sci. Technol.* **17**, 1028 (1980); Wang Y. and Joannopoulos J. D., *J. Vac. Sci. Technol.* **17**, 997 (1980).
- Chadi D. J. and Cohen M. L., *Phys. Stat. Solidi* **68**, 405 (1975).
- Chelikowsky J. R. and Cohen M. L., *Phys. Rev.* **14**, 556 (1976).
- The primitive vectors of the zincblende (fcc) lattice are

$$\mathbf{A}_1 = (a_L/2)(1, 1, 0),$$

$$\mathbf{A}_2 = (a_L/2)(0, 1, 1),$$

and

$$\mathbf{A}_3 = (a_L/2)(1, 0, 1),$$

where a_L is the lattice constant. The primitive vectors of the bcc reciprocal space are

$$\mathbf{a}_1 = (2\pi/a_L)(1, 1, -1),$$

$$\mathbf{a}_2 = (2\pi/a_L)(-1, 1, 1),$$

and

$$\mathbf{a}_3 = (2\pi/a_L)(1, 1, 1).$$

The wavevectors of the first Brillouin zone are

$$\mathbf{k} = (2\pi/a_L)(u_1, u_2, u_3),$$

$$\text{with } u_1 + u_2 + u_3 \leq 3/2.$$

The positions of the four atoms nearest to a central anion are

$$\mathbf{v}_1 = (a_L/4)(1, 1, 1),$$

$$\mathbf{v}_2 = (a_L/4)(-1, 1, -1),$$

$$\mathbf{v}_3 = (a_L/4)(1, -1, -1),$$

and

$$\mathbf{v}_4 = (a_L/4)(-1, -1, 1),$$

and the positions of the anions in the twelve nearest unit cells are given by the non-zero combinations of $\mathbf{v}_i - \mathbf{v}_j$ for $i, j = 1, 4$.

14. The Löwdin orbitals are

$$|nb\mathbf{R}_i\rangle = \sum_{m, \mathbf{v}_b} S^{-1}(nb\mathbf{R}_i, m\mathbf{b}'\mathbf{R}_i)a(m\mathbf{b}'; \mathbf{r} - \mathbf{R}_i - \mathbf{v}_b),$$

where $a(m\mathbf{b}'; \mathbf{r} - \mathbf{R}_i - \mathbf{v}_b)$ is an atomic orbital with quantum numbers m centered at $\mathbf{R}_i + \mathbf{v}_b$. The overlap matrix elements are

$$S(nb\mathbf{R}_i, m\mathbf{b}'\mathbf{R}_i) = \int d^3r a^*(nb; \mathbf{r} - \mathbf{R}_i - \mathbf{v}_b)a(m\mathbf{b}'; \mathbf{r} - \mathbf{R}_i - \mathbf{v}_b).$$

By using Löwdin orbitals instead of atomic orbitals, we obtain a secular equation of the form $\det(\epsilon - H) = 0$ instead of one with the troublesome overlaps: $\det(\epsilon S - H) = 0$. See Löwdin P. O., *J. Chem. Phys.* **18**, 365 (1950).

- The following matrix elements have been set equal to zero: $(s^*a\mathbf{R}|H|s^*c\mathbf{R})$, $(s^*a\mathbf{R}|H|sc\mathbf{R})$, and $(sa\mathbf{R}|H|s^*c\mathbf{R})$.
- Hjalmarson H. P., Ph.D. Thesis, University of Illinois (1979).
- Hjalmarson H. P., Vogl P., Wolford D. J. and Dow J. D., *Phys. Rev. Letters* **44**, 810 (1980).
- The eigenvalue equation for an energy level associated with a localized defect has significant, partially cancelling contributions from states ± 10 eV from the fundamental band gap, as shown in Ref. [17]; thus an accurate knowledge of the density of states over a 20 eV range is needed.
- To calculate the local density of states, we use a special-points tetrahedral-volume method based on the ideas of Lehman G. and Taut M., *Phys. Stat. Solidi* (b) **54**, 469 (1972); the FORTRAN program is listed in Ref. [16].
- Ham F. S., *Solid. St. Phys.* **1**, 127 (1955) [Seitz F. and Turnbull D. (Eds.), Academic Press, New York (1955)].
- Abarenkov I. V. and Heine V., *Phil. Mag.* **12**, 529 (1965); Heine V. and Abarenkov I. V., *Phil. Mag.* **9**, 451 (1964).
- The matrix elements $V(s^*a, pc)$ and $V(pa, s^*c)$ are obtained by fitting the Hamiltonian in eqn (5) to the X -point data at X_1^c and X_3^c . To do this, all other matrix elements are left unchanged, and $V(s^*a, pc)$ is determined by setting to zero the determinant that originates from one of the two three by three block matrices within the Hamiltonian:

$$[E(s^*, a) - E(X_1^c)][(E(s, a) - E(X_1^c))(E(p, c) - E(X_1^c)) - V(s^*a, pc)^2] - V(sa, pc)^2(E(s, a) - E(X_1^c)) = 0.$$

The matrix element $V(pa, s^*c)$ is obtained from the corresponding equation for $E(X_3^c)$.

- Ley L., Pollak R. A., McFeely F. R., Kowalczyk S. P. and Shirley D. A., *Phys. Rev.* **B9**, 600 (1974).
- Experiments have not been reported for these interfaces, but Ref. [3], p. 253, predicts a valence band discontinuity of about 2.0 eV for both of these heterojunctions.
- Hjalmarson H. P., Buttner H. and Dow J. D., *Phys. Lett* **85A**, 293 (1981); *Phys. Rev.* **B24**, 6010 (1981).

26. Allen R. E., Hjalmarson H. P., Vogl P., Wolford D. J., Sankey O. F. and Dow J. D., *Int. J. Quantum Chem., Quantum Chem. Symp.* 14, 607 (1980).
27. Hjalmarson H. P., Allen R. E., Büttner H. and Dow J. D., *J. Vac. Sci. Technol.* 17, 993 (1980).
28. Allen R. E., Hjalmarson H. P. and Dow J. D., *Surface Sci.* 110, L625 (1981).
29. Allen R. E., Buisson J. P. and Dow J. D., *Appl. Phys. Lett.* 39, 975 (1981).
30. Allen R. E. and Dow J. D., *Phys. Rev. B* 25, 1423 (1982); *Appl. Surface Sci.* 11/12, 362 (1982); Dow J. D. and Allen R. E., *J. Vac. Sci. Technol.* 20, 659 (1982).
31. Sankey O. F., Hjalmarson H. P., Dow J. D., Wolford D. J. and Streetman B. G., *Phys. Rev. Letters* 45, 1656 (1980).
32. Fisher C. E., *Atomic Data* 4, 301 (1972); see also Clementi E. and Roetti C., *Atomic Data and Nuclear Tables* 14, 177 (1974).
33. Moore C. E., *Atomic Energy Levels*, National Bureau of Standards Circular 467. U.S. Government Printing Office, Washington, D.C. (1949).
34. When a_L is infinite, α_1 vanishes.
35. For example, see Jennison D. R., *Phys. Rev.* B16, 5147 (1977).

APPENDIX A

Semiconductor bandstructures

Figures 11 give the sp^3s^* band structures (solid lines) of the various zincblende semiconductors, in comparison with the pseudopotential band structures [12] when available (dashed lines).

APPENDIX B

Determination of β_1

An approximation D_p^0 to the difference D_p in the diagonal matrix elements for p orbitals can be extracted from data using a relationship [11] among D_p , the Γ_{15} conduction band energy, the spin-orbit splitting Δ_0 of the highest two valence bands, and the atomic spin-orbit splittings of the anion and cation Δ_a and Δ_c :

$$D_p^0 = (2\Delta_0 - \Delta_a - \Delta_c)E(\Gamma_{15}^c)/(\Delta_a - \Delta_c). \quad (B1)$$

By plotting D_p^0 vs the neutral atom energy difference $w(p, c) - w(p, a)$ for several semiconductors we find the average value 0.6 for $\beta_p = D_p^0/(w(p, c) - w(p, a))$. (See Fig. 8 and Table 3.)

Exploiting the relationship obtained from the Hamiltonian for energies at the X point

$$E(s, c) - E(s, a) = E(p, c) - E(p, a) + E(X_3^s) - E(X_1^s) + E(X_3^c) - E(X_3^a),$$

and plotting the r.h.s., while using D_p^0 for $E(p, c) - E(p, a)$, against $w(s, c) - w(s, a)$, we find $\beta_s = 0.8$ (Fig. 9).

APPENDIX C

The s and p orbital energies were obtained from Hartree-Fock calculations for neutral atoms [32]. The s^* orbital energies were obtained from tabulated spectroscopic data [33]. Associated with each p orbital in a term of angular momentum J was a transition energy; an average energy was obtained by weighting each transition energy by a multiplicity factor of $2J + 1$.

APPENDIX D

Orbital energies within the solid

The Lowdin orbital of symmetry l on a specific site is composed primarily of the atomic orbital at that site with a slight admixture from neighboring sites. The component from an orbital at a neighboring site depends on its overlap with the primary orbital; this overlap decreases sufficiently rapidly with distance that to a good approximation we can ignore the effect of all but the nearest neighbor atoms. In the spirit of this model, we assume that the diagonal matrix elements are functions of the

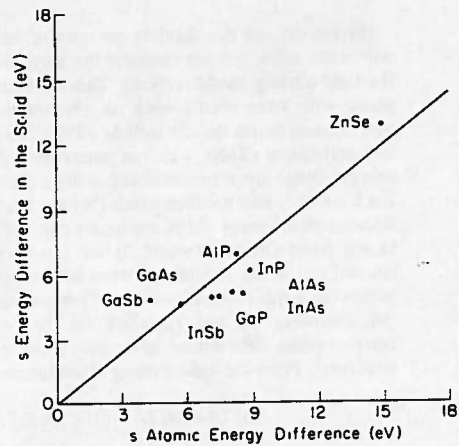


Fig. 9. The s -orbital energy differences, obtained in terms of the X -point energy differences (see eqn B2) vs the s -orbital energy differences in the neutral atom. The slope of the dashed line is $\beta_s = 0.8$.

atomic energies, and we make the linear approximation

$$E(1, a) = w(1, a) + \alpha_1 w(1, c) \quad (D1)$$

$$E(1, c) = w(1, c) + \alpha_1 w(1, a) \quad (D2)$$

to relate the energies in the solid, $E(1, b)$, to neutral atom orbital energies $w(1, b)$ of Table 3 ($b = a$ for the anion and $b = c$ for the cation). The coefficients α_1 , representing the admixture of the nearest neighbor, are small, and depend on the symmetry l and the lattice constant a_L . In our crude model we ignore their dependence on lattice constant [34].

The diagonal energies enter the calculation as sums S_l and differences D_l which are defined by the atomic energies:

$$S_l = E(1, c) + E(1, a) = (1 + \alpha_1)(w(1, c) + w(1, a)), \quad (D3)$$

and

$$D_l = E(1, c) - E(1, a) = (1 - \alpha_1)(w(1, c) - w(1, a)). \quad (D4)$$

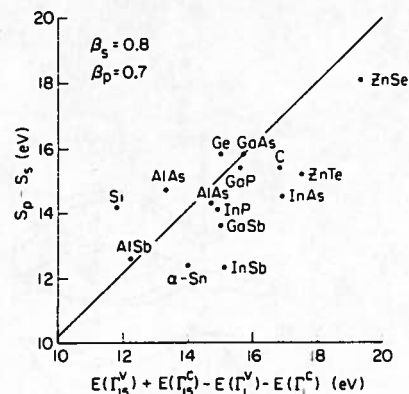


Fig. 10. Shows the relationship of orbital energies in the solid to neutral atom orbital energies. See eqn (D6). The fact that the points cluster along the diagonal of the figure indicates that the sums of the anion and cation orbital energy differences, obtained from the "universal" model (see eqns D1 and D2), agree with those directly determined from the experimental band structure. Here we use $\beta_p = 0.7$; in Fig. 9 we would find a better fit with $\beta_p = 0.5$. Thus we settle on the average value of 0.6.

Having defined the absolute energies of tight-binding orbitals within the solid, we can compute the corresponding energies of the tight-binding bandstructures. These cannot be directly compared with experiments such as photoemission, because the tight-binding bands do not include effects, mainly electron-electron correlation effects, which in general shift the bands to higher energy. Other more sophisticated methods, such as the Hartree Fock method, also produce bands that are too low in energy [35]. Because such energy shifts are nearly constant, as demonstrated by the Bond Orbital Model [2, 3], we can construct an indirect, internal test of the absolute energies of the tight-binding orbitals within the solid. The test consists of computing the differences of two quantities, S_p and S_s , which are then compared with the corresponding differences computed from experimental band structures. From the tight-binding Hamiltonian we obtain

$$E(\Gamma_{15}^+) + E(\Gamma_{15}^-) - E(\Gamma_1^+) - E(\Gamma_1^-) \quad (D5)$$

for $S_p - S_s$ derived from bandstructure. In Fig. 10, that quantity is shown to compare favorably with

$$S_p - S_s = (2 - \beta_p)(w(p, c) + w(p, a)) - (2 - \beta_s)(w(s, c) + w(s, a)) \quad (D6)$$

obtained from eqns (D3) and (D4), using $\beta_i = 1 - \alpha_i$.

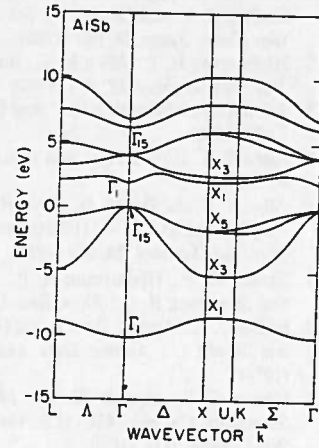


Fig. 11(c)

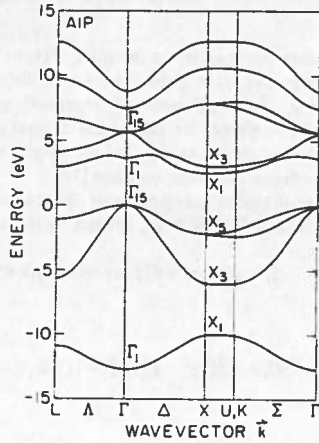


Fig. 11(a)

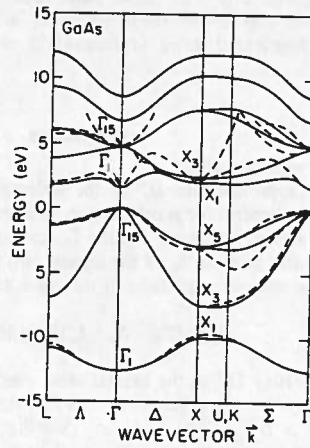


Fig. 11(d)

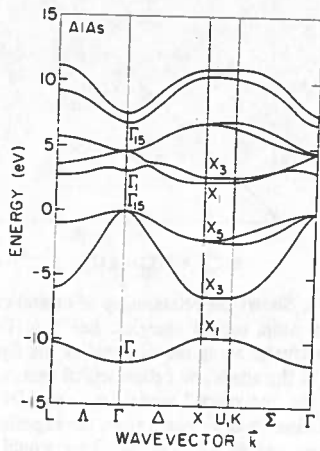


Fig. 11(b)

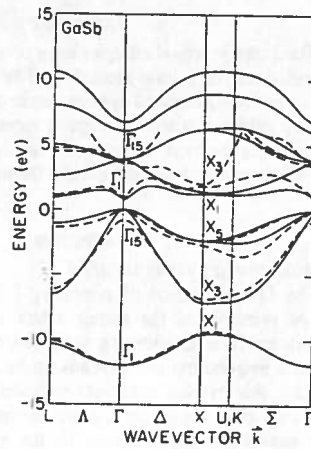


Fig. 11(e)

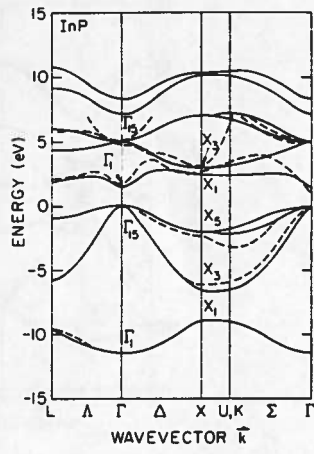


Fig. 11(f).

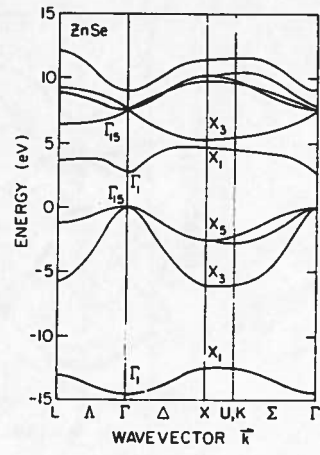


Fig. 11(i).

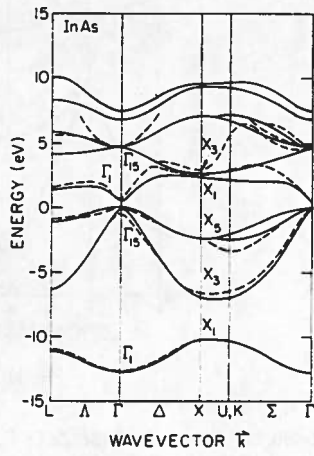


Fig. 11(g).

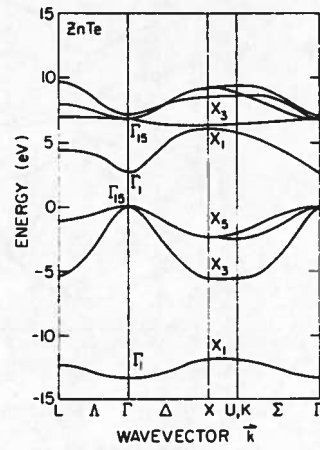


Fig. 11(j).

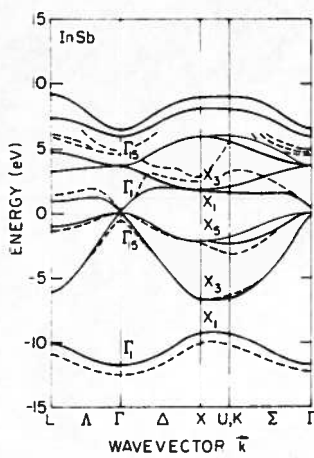


Fig. 11(h).

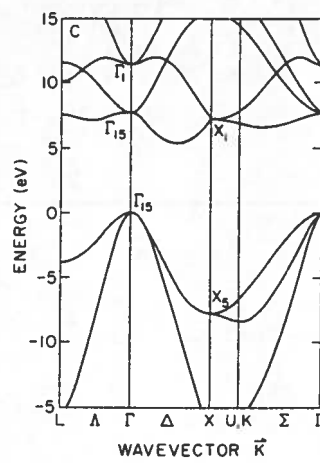


Fig. 11(k).

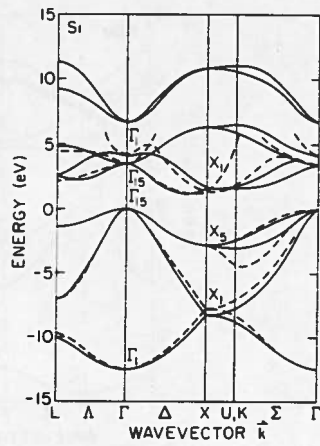


Fig. 11(l).

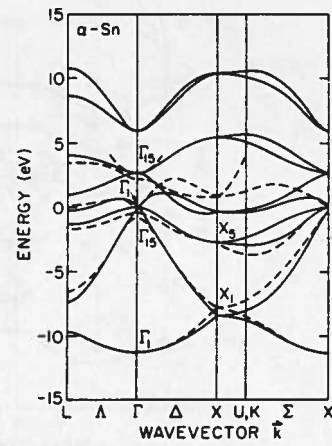


Fig. 11(n).

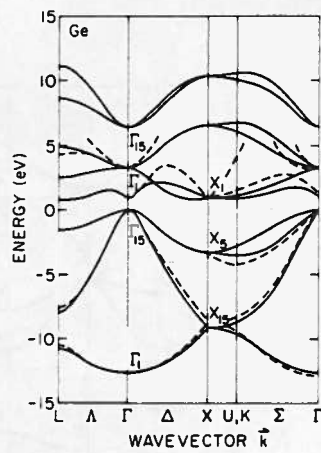


Fig. 11(m).

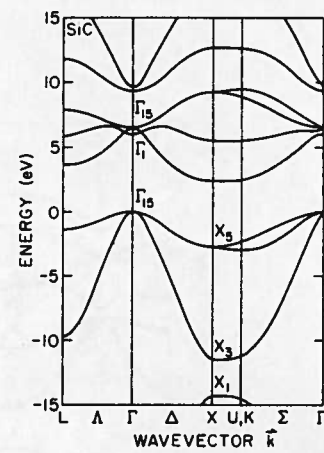


Fig. 11(o).

Fig. 11. The sp^3s^* band structures for AlP, AlAs, AlSb, GaAs, GaSb, InP, InAs, InSb, ZnSe, ZnTe, C, Si, Ge, Sn, and SiC. For simplicity, the symmetry points that were fit to experimental data are labelled with a uniform non-relativistic zincblende notation, even for diamond-structure crystals. A non-local pseudopotential band structure (dashed line) is included whenever one is available [12].